Journal of Hazardous Materials, 31 (1992) 39–57
Elsevier Science Publishers B.V., Amsterdam

Leaching of simulated heavy metal waste stabilized/solidified in different cement matrices

R.B. Heimann[a,c], D. Conrad[b], L.Z. Florence[b], M. Neuwirth[b], D.G. Ivey[c], R.J. Mikula[d] and W.W. Lam[d]

[a]*Alberta Research Council, Edmonton, Alberta, T6H 5X2 (Canada)*
[b]*Alberta Environmental Center, Vegreville, Alberta, T0B 4L0 (Canada)*
[c]*University of Alberta, Department of Mining, Metallurgical and Petroleum Engineering, Edmonton, Alberta, T6G 2G6 (Canada)*
[d]*Energy, Mines and Resources Canada (CANMET), Devon, Alberta, T0C 1E0 (Canada)*

(Received August 10, 1991; accepted in revised form November 29, 1991)

Abstract

Leaching experiments have been carried out on samples of ordinary portland cement (OPC), sulphate-resistant portland cement (SRPC) with fly ash (FA) added and an alumina cement (AC), with each receiving various concentrations (0.1–1.0 *M*) of chromium (Cr^{6+}), vanadium (V^{5+}) and cadmium (Cd^{2+}). The samples were prepared and evaluated with a statistical experimental matrix corresponding to a Box–Behnken fractional factorial design. Leaching was done in PTFE vessels using the standard TCLP (toxicity characteristic leaching procedure of the U.S. Environmental protection Agency). Analyses of the leachates were carried out for elements Cr, Cd, V, Si, Al, Ca and Fe by inductively coupled plasma spectroscopy. Selected solid samples were investigated before and after leaching by scanning electron microscopy, in conjunction with energy dispersive X-ray spectrometry, and by scanning transmission electron microscopy on thinned specimens. The normalized mass losses of chromium varied between $3.3\ 10^{-2}$ and $3.5\ 10^{-1}$ kg/m^2. Calculated maximum release was found for a hypothetical cement with approximately 20% alumina, while minimum release was found for AC with 36.7% alumina. The normalized mass losses of vanadium varied between $1\ 10^{-3}$ and $8\ 10^{-2}$ kg/m^2. Calculated maximum release was found for a hypothetical cement with approximately 25% alumina and minimum release was found for OPC. All samples of the cadmium series except three showed solution concentrations below the detection limit (0.1 ppm), suggesting very effective retention of this element by all three cement matrices investigated.

1. Introduction

The Alberta Hazardous Waste Regulations identify hazardous wastes in accordance with a variety of criteria including the Transportation of Dangerous Goods Act. The regulated contaminants include cadmium, chromium and vanadium. These elements are contained in a variety of industrial wastes generated in Alberta.

Correspondence to: Dr. R.B. Heimann, Alberta Research Council, Edmonton, Alberta, T6H 5X2, Canada.

0304-3894/92/$05.00

Stabilization/solidification typically involves the physical entrapment and/or chemical binding of toxic elements or compounds in a stable matrix. This reduces significantly the exposed surface area of the waste, thereby reducing the mobility and leachability of the toxic elements into the groundwater and surface waters. Most processes applied to aqueous wastes are cement-based (ordinary portland cement, OPC) and use additives such as fly ash or kiln dust.

Several approaches have been used in the past to study the mechanism of containment of hazardous wastes (heavy metals) in stabilized/solidified products. Results from leaching studies generally agree that pH is the major controlling factor in the leachability of waste metals from stabilized/solidified products [1–4]. Chromium, cadmium and lead have different leaching characteristics when leached by different tests. The concentration of the metals (Cr, Cd, Zn and Hg) in the leachate is lower than predicted based on their hydroxide solubilities, indicating that they are strongly bound to the matrix and are only released when the latter is destroyed [2].

Scanning and transmission electron microscopy (SEM and TEM) and X-ray diffraction studies have shown that the morphology of the solid hydration products of OPC is modified when certain metals such as Cr are added [5–7]. Cement hydration accelerators, such as Cr^{3+}, are chemically incorporated into all phases of hydrated OPC, suppressing ettringite formation. Chromium appears to substitute for silicon in calcium silicate hydrates (C-S-H) as well as being associated with regions of high calcium content such as $Ca(OH)_2$ and $Ca(NO_3)_2$ [7].

The objective of the present paper is to increase our understanding of the mechanism of containment of the heavy metals chromium, vanadium and cadmium in cementitious matrices. Different mechanisms of containment have been suggested for these metals [6,8,9].

To predict the integrity of the containment system over the long term, mathematical models are being developed which are based on the results of leaching experiments in the laboratory. However, extrapolation of these data, and generalization of the conclusions of short-term leaching studies, will require knowledge of the mechanisms of containment. Thus, research into this area is timely and warranted.

2. Experimental methods

2.1 Sample preparation, leaching tests and analysis

Metal solutions (0.1, 0.4, 1.0 *M*) were prepared from cadmium nitrate ($Cd[NO_3]_2 \cdot 4H_2O$; Fisher Scientific certified grade) chromium trioxide (CrO_3), (BDH Chemicals; 99% purity), sodium orthovanadate (Na_3VO_4), (Aldrich Chemicals) and ASTM Type I H_2O.

The cements used were: ASTM I ordinary portland cement (OPC, Canada

TABLE 1

Composition of the cements and fly ash

Chemical compound	OPC	AC	SRPC	FA
Oxides (wt%)				
CaO	62.16	36.74	62.58	14.06
MgO	4.02	0.29	3.92	1.30
Na_2O	0.18	0.02	0.17	2.90
K_2O	0.59	0.03	0.61	0.51
Al_2O_3	3.75	36.73	3.06	20.13
Fe_2O_3	2.53	16.30	3.76	3.43
TiO_2	0.18	1.82	0.17	0.54
SiO_2	20.33	3.74	21.23	51.68
Elements (wt%)				
S	0.68	0.01	0.62	0.10
V	0.01	0.04	0.01	0.01
Cr	0.01	0.07	0.01	0.01

Cement Lafarge); a 70/30 vol% mixture of sulphate-resistant portland cement (SRPC, Canada Cement Lafarge) and Classified Type "C" Fly ash (FA, Western Canada Fly Ash); and alumina cement (AC, Ciment Fondu Canada Cement Lafarge). The cement compositions are shown in Table 1.

The various metal solutions were combined with 800.0 ± 0.1 g of cement yielding cement pastes of approximately 1 kg mass. The range of final metal concentration was 1000–12 000 mg/kg for Cr, 1000–12 000 mg/kg for V and 2200–27 000 mg/kg for Cd. Samples were mixed for 5 min in a Hobart Model M50 mixer operating at 131 rotational rpm and 61 planetary rpm. Samples were formed in Teflon-lined mortar molds, 50 mm on edge, and cured at the design temperatures of 25, 50 and 75 °C and 98% relative humidity in an environmental chamber (Tabai Espec Corporation Model PLIG) for 7, 36 or 60 days. On completion of curing, the samples were crushed. The fraction passing a 9.5 mm screen and retained on a 4.8 mm screen was used for leaching studies. This relatively narrow range of particle sizes was selected to permit estimation of geometric surface area, necessary for determination of normalized mass losses during leaching.

Leaching solutions of 0.1 *N* acetic acid were prepared and sample leachates were obtained according to the U.S. EPA's TCLP [10]. Leachate pH was measured prior to acidification with 1 vol% 8 *N* nitric acid. Leachate metal analyses (Cr, Cd, V, Al, Si, Ca, Fe) were performed by inductively coupled plasma spectroscopy (ARL model 3400).

2.2 *Experimental design and analysis*

Many independent parameters influence the performance of an actual waste containment system based on cementitious materials. Thus, in order to reduce

the large number of experiments required to accommodate a large number of parameters, an appropriate and economical statistical design is needed.

Fourteen parameters were tentatively identified, which can potentially control the amount of hazardous heavy metal elements released from the solidified cementitious waste during leaching. These parameters are listed in Table 2. Parameters X_5 to X_{14} were kept constant for all experiments at the levels shown in Table 2. Their values were consistent with the requirements of the TCLP test. Parameters X_1 (type of cement matrix), X_2 (concentration of waste element), X_3 (curing temperature of cement paste) and X_4 (curing time of cement paste) were varied at the levels indicated in Table 2 for the selected elements Cr, V and Cd. The statistical matrix chosen to yield the most information per unit effort corresponded to a four-factor fractional factorial Box–Behnken type design [11] with each factor at three levels. One set of experiments consisting of 27 runs was conducted for each of the heavy metals Cr, V and Cd. In order to avoid systematic experimental error progression, the 81 runs were randomized. From the measured concentrations of Cr, V and Cd in the leachates, normalized mass losses (NML) were calculated. Similarly, NML for aluminum in the leachates were calculated in order to simultaneously determine the varying solubilities of Al in the cement matrices. These data were

TABLE 2

Test parameter matrix

Parameter X	Factors	Units	Uncoded levels		
1	Type of matrix	% Al_2O_3	3.75 (OPC)	7.11 (S+F)	36.73 (AC)[a]
2	Concentration	mol/l	0.1	0.4	1.0
3	Curing temperature	°C	25	50	75
4	Curing time	days	7	36	60
5	Curing moisture	% RH		98 ± 2	
6	Mass of cement	g		100 ± 0.1	
7	Water/cement ratio	g/g		0.234–0.298	
8	Surface/volume	m^{-1}		0.13	
9	Type of leachant	—		0.1 *N* acetic acid	
10	Leach time	h		18	
11	Leach temperature	°C		23 ± 2	
12	Liquid/solid ratio	ml/g		20	
13	Type of agitation	—		Rotary extractor	
14	Type of leach test	—		TCLP[b]	

[a]OPC: Ordinary portland cement (Canada Cement Lafarge Ltd);
S: Sulphate resistant portland cement (Kalicrete, Type 50; Canada Cement Lafarge Ltd);
F: Fly ash (Western Canada Flyash). Ratio S/F = 70/30 vol%;
AC: Aluminous cement (Ciment Fondu R1; Canada Cement Lafarge Ltd).
[b]TCLP: Toxicity characteristic Leaching Procedure (U.S. EPA).

chosen as dependent response variables in estimates of second-degree polynomial coefficients using the regression methods contained in the RSREG statistical routines (SAS 1988 release 6.03) [12].

2.3 Electron microscopy

Both unleached and leached specimens were examined by electron microscopy. Specimens for transmission and scanning transmission electron microscopy (TEM/STEM) were prepared using a combined dimpling/ion milling process similar to that described by Ivey et al. [7]. A 1–2 mm thick slice was cut from the cured material using a low speed diamond saw, followed by cleaning in acetone. Discs, 3 mm in diameter, were machined from this slice, using an ultrasonic disc cutter. The discs were mechanically polished from both sides to a thickness of 150–250 μm. Specimens were dimpled on one side, down to a central thickness of about 70 μm, using 0.25 μm diamond paste. The other side was then dimpled until a small hole appeared. Specimens were thoroughly rinsed in acetone, followed by rinsing in ethanol, and then bonded to copper rings, for durability and support, with a two-part rapid-setting epoxy. Specimens were ion milled for 1.5–2 h, using Ar as the sputtering species, at a potential of 4–5 kV, a current of $\cong$0.5 mA/gun and an incidence angle of 18° to the horizontal. Carbon-coated specimens were then examined in an Hitachi H-600, 100 kV TEM/STEM equipped with a Kevex Be window X-ray detector.

A Hitachi X-650 scanning electron microscope (SEM), equipped with both wavelength and energy dispersive X-ray spectrometers, was also used for this study. The SEM is coupled to a Tracor 8502 image analyzer via a Tracor 5400 X-ray analyzer. This allows for control of the microscope by the X-ray analyzer and for automated data collection. Samples were prepared by fracturing and leached cement samples and choosing a fracture surface that was relatively flat. Backscattered electron images are useful in determining areas of differing atomic number and were acquired in this case with a GW Electronics solid-state detector mounted directly on the pole piece.

3. Results and discussion

3.1 Normalized mass losses of chromium, vanadium and aluminum

From the concentrations of Cr, V and Cd in the leach solutions, normalized mass losses (in kg/m^2) were calculated according to [13]

$$NML_i = (c_i V / c_i^0)/SA \quad (1)$$

where c_i denotes the concentration of element i in the leach solution in mg/l, c_i^0 the concentration of element i in the solid in mg/kg, V the volume of the leach solution in litre, and SA the surface area of the solid in m^2, calculated assuming a geometric solid of fixed size.

The data were corrected for the amounts of Cr and V contained in the orig-

inal cements (Table 1), and for the varying amounts of metal solutions added to make up the cement paste. It is evident from Table 3, with a few exceptions, that the solution concentrations of Cd were below the detection limit.[1]

Plots of *NML*(Al) vs. pH for leachate solutions generated by AC, SRPC+FA and OPC, all doped with Cr, V and Cd are shown in Figs. 1(a–c). For AC (Fig. 1(a)), *NML*(Al) for V-containing cement is a significant ($P<0.05$) quadratic function of pH; 93% of the variation in *NML*(Al) is explained by the quadratic model. *NML*(Al) is minimized between pH 7.0 and 9.0 and hence exhibits amphoteric character, existing in solution as Al^{3+} ion below pH 7 and

TABLE 3

Normalized mass losses (NML_i) in kg/m^2 for chromium, vanadium and cadmium

Chromium			Vanadium			Cadmium		
Trial #	*NML*(Cr)	*NML*(Al)	Trial #	*NML*(V)	*NML*(Al)	Trial #	*NML*(Cd)	*NML*(Al)
12	0.240	0.0040	39	0.011	0.003 30	66	—	0.0043
24	0.160	0.0075	51	—	0.006 80	78	—	0.0071
13	0.200	0.0038	40	0.006	0.003 70	67	—	0.0037
4	0.071	0.0058	31	—	0.005 30	58	—	0.0053
15	0.140	0.0061	42	0.001	0.005 90	69	—	0.0068
25	0.063	0.0370	52	0.001	0.022 00	79	—	0.0039
14	0.066	0.0440	41	—	0.000 93	68	—	0.0053
26	0.140	0.0061	53	0.001	0.005 70	80	—	0.0064
22	0.191	0.0036	49	0.012	0.003 60	76	—	0.0038
16	0.046	0.0290	43	0.002	0.005 40	70	—	0.0029
27	0.210	0.0036	54	0.040	0.003 60	81	—	0.0039
20	0.033	0.0100	47	0.077	0.260 00	74	0.027	0.0083
5	0.230	0.0041	32	0.037	0.003 80	59	—	0.0045
7	0.150	0.3000	34	0.074	0.30 000	61	0.049	0.0039
6	0.200	0.0036	33	0.007	0.003 80	60	—	0.0039
23	0.055	0.0430	50	—	0.000 74	77	—	0.0037
21	0.240	0.0044	48	0.002	0.003 70	75	—	0.0043
11	0.190	0.0041	38	0.025	0.004 50	65	—	0.0042
17	0.160	0.0062	44	0.002	0.003 70	71	—	0.0071
18	0.220	0.0039	45	0.038	0.005 70	72	—	0.0053
10	0.240	0.0044	37	0.037	0.003 70	64	—	0.0046
2	0.042	0.0440	29	0.036	0.039 00	56	—	0.0056
3	0.160	0.0058	30	0.002	0.007 10	57	—	0.0093
1	0.100	0.0007	28	0.002	0.001 00	55	—	0.0058
19	0.350	0.0039	46	0.068	0.210 00	73	0.240	0.0079
8	0.190	0.0043	35	0.002	0.004 40	62	—	0.0049
9	0.210	0.0036	36	0.032	0.003 50	63	—	0.0038

[1]A comprehensive list of the leachate analyses data, including leachate pH, is available from the first author on request.

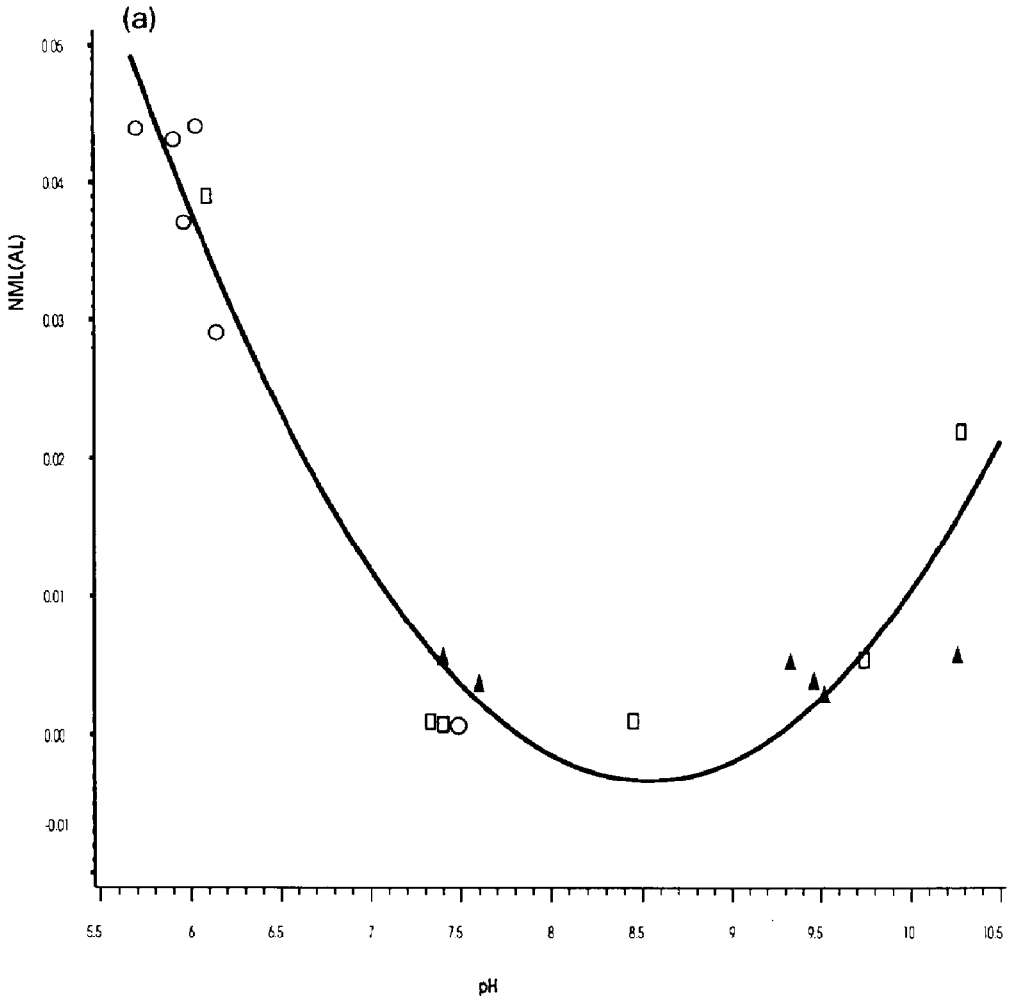

Fig. 1(a). Normalized mass loss of Al vs. pH for aluminous cement doped with Cr (○), V (□)) and Cd (▲).

$[Al(OH)_4]^-$ above pH 9. Apparently, for V-containing alumina cements, the chemistry of the cements is controlled by the solution chemistry of aluminum. For Cr-containing cements, the pH never increases above 7.5 in the experimental region observed. On the other hand, Cd-containing cements do not show pH data below 7.4.

For SRPC + FA (Fig. 1(b)), *NML*(Al) data occupy a narrow band between $3.3\ 10^{-3}$ and $5.7\ 10^{-3}$ kg/m^2 for pH > 6.9, corresponding to an average $[Al^{3+}]$ solution concentration of $10^{-3.62}$ mol/l. Below a pH of 6.9, aluminum release from SRPC + FA increases sharply for Cr and V, but not for Cd. The constancy of *NML*(Al) for pH > 6.9 suggests that the concentration of aluminum in solution is being controlled by the solubility of a sparingly soluble aluminum

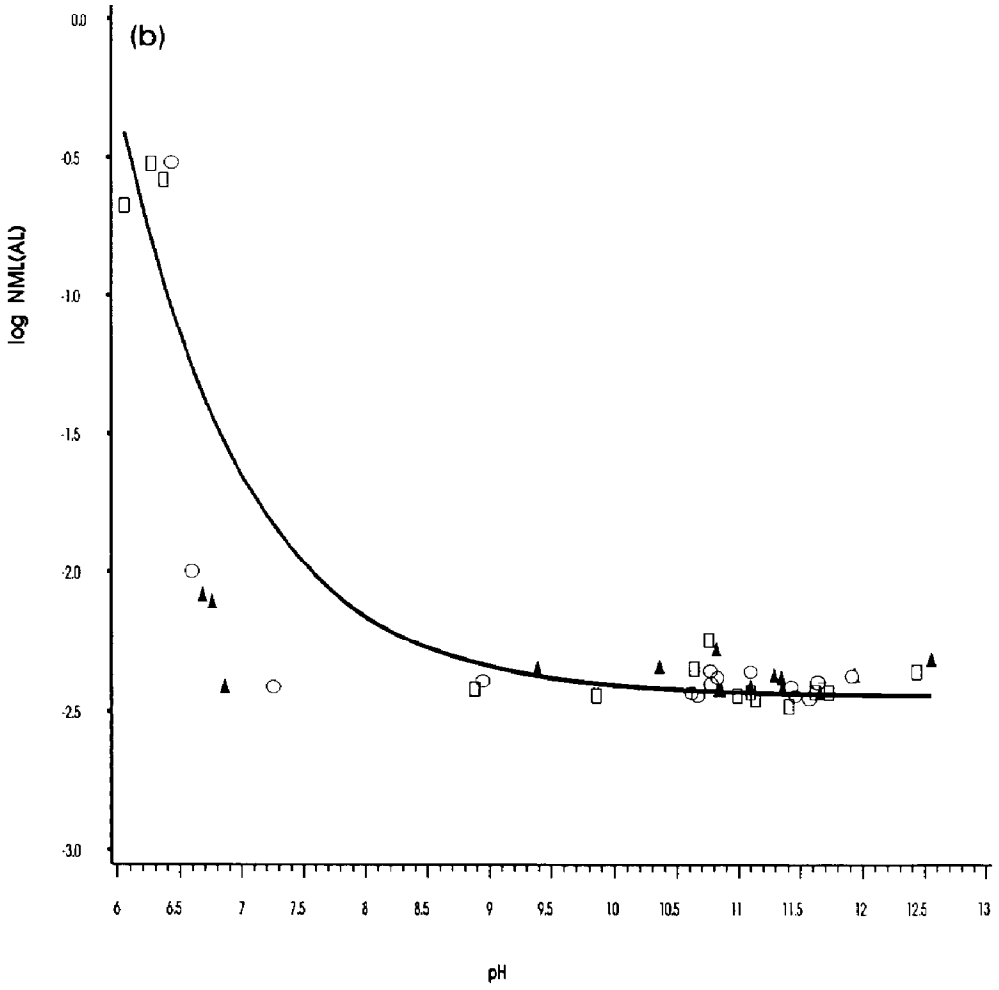

Fig. 1(b). Normalized mass loss of Al vs. pH for sulfate-resistant portland cement+fly ash, SRPC+FA. Symbols as in Fig. 1(a).

compound. The negative power function shown in Fig. 1(b) explains 75% ($r^2=0.75$) of the variation in log NML(Al). In contrast to the high-aluminous AC, the chemistry of the cement is also influenced by other elements. The results of geochemical modeling using appropriate equilibrium codes to ascertain the nature of the phase controlling aluminum levels in solution will be shown in a forthcoming paper.

Figure 1(c) shows NML(Al) vs. pH for OPC, in which the slope is not different from zero for any of the metals, indicating that NML(Al) varies randomly with varying pH levels. The pH of the leach solutions obtained from OPC always exceeds 10, due to $Ca(OH)_2$ produced on hydration. The NML(Al) values vary between 5 10^{-3} and 9.5 10^{-3} kg/m^2, and are thus slightly higher than those found for the SRPC+FA cement (see Fig. 1(b)). The average [Al^{3+}] solution concentration is $10^{-3.57}$ mol/l.

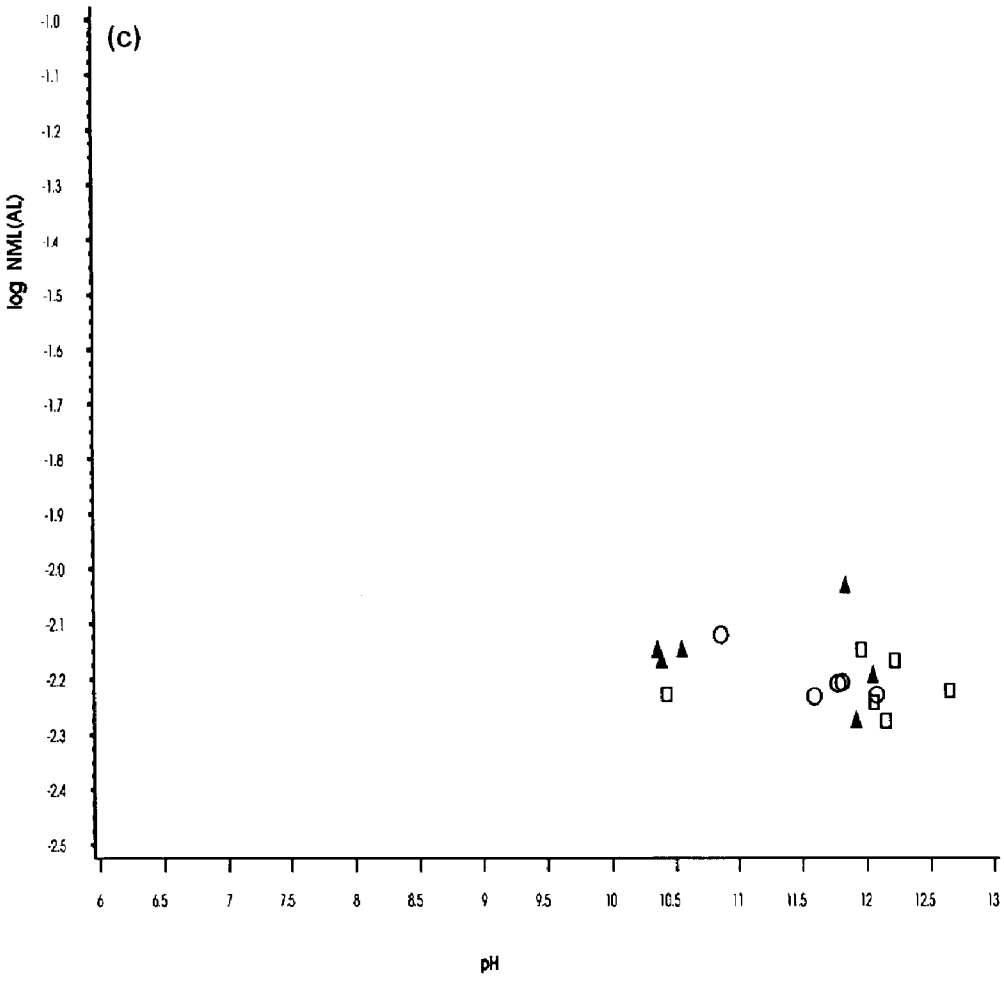

Fig. 1(c). Normalized mass loss of Al vs. pH for ordinary portland cement, OPC. Symbols as in Fig. 1(a).

From Figs. 1(a–c), it appears that the retention of Al in the Cd-containing cements is not dependent on pH. This suggests a strong interaction between Cd and Al in all cements containing Cd.

3.2 Response surface models

Results of regressions of NML(Cr), (V), (Al) and pH for Cr and V are summarized in Table 4. In each case, the following polynomial model[2] was fitted to the data by the method of least squares regression analysis:

$$y = b_0 + b_1 x_1 + b_2 x_2 + b_3 x_3 + b_4 x_4 + b_{11} x_1^2 + b_{22} x_2^2 + b_{33} x_3^2 + b_{44} x_4^2 + b_{12} x_1 x_2 + b_{13} x_1 x_3 + b_{14} x_1 x_4 + b_{23} x_2 x_3 + b_{24} x_2 x_4 + b_{34} x_3 x_4 \quad (2)$$

[2]The four three-factor interactions and the four-factor interaction have been omitted.

TABLE 4

Summary of response surface regression analyses (coded data) with a Box–Behnken design matrix[a] having four independent factors: Cement matrix, metal ion concentration, curing temperature and curing time, each at three levels. The variation explained by the unreduced model is shown by r^2 and $Pr > F$ is the level at which α, or Type I error, can be set

Y	b_0	b_1	b_2	b_3	b_4	b_{11}	b_{12}	b_{13}
$NML(\mathrm{Cr}) \times 10^2$	34.44	*−4.17*	4.11	0.35	1.64	*−22.02*	−1.14	−0.87
$NML(\mathrm{V}) \times 10^2$	11.79	*1.53*	−0.50	1.64	3.08	*−10.45*	*−1.38*	1.73

b_{14}	b_{22}	b_{23}	b_{24}	b_{33}	b_{34}	b_{44}	r^2	$Pr > F$
1.36	−2.40	−0.04	*5.73*	−0.37	1.49	−1.01	0.88	0.001
0.71	−1.22	0.54	1.16	−0.61	−0.97	0.07	0.90	0.025

[a]Italic figures: Coefficient differs from 0 at $\alpha = 0.05$ or less, b_0 = intercept, b_1 = cement matrix, b_2 = metal concentration, b_3 = curing temperature, b_4 = curing time and b_{ij} = two-factor interactions.

Normalized mass losses of Cr were significantly related to the cement matrix and the two-factor interaction of the concentration (X_2) and the curing time (X_4) with both linear and quadratic terms of the former retained in the model. The relationship is shown in Figs. 2(a) and 3(a). Curing temperature is fixed at 25°C and curing time is fixed at 8 days in Fig. 2(a), while concentration (X_2) is fixed at 5157 mg/l and curing temperature (X_3) is fixed at 17°C in Fig. 3(a). Mobility of Cr was restricted most at low and high alumina contents of the cement matrix. Contour plots of $NML(\mathrm{Cr})$ projected onto the matrix-concentration plane and the matrix-curing time plane are shown in Figs. 2(b) and 3(b), respectively. The parabolic relationships point to a strong matrix effect that is manifest in the control of the leachability of Cr by the level of Al in the cement. The reason for this matrix effect will be an area for further study.

In addition, $NML(\mathrm{V})$ was found to exhibit significant linear and quadratic responses to cement matrix (Fig. 4(a)), and the two-factor interaction of the cement matrix (X_1) and the concentration of added V (X_2) were also retained in the model (Table 4). $NML(\mathrm{V})$ was lowest when alumina was present in the cement matrix at 3.75% (OPC) and maximized at intermediate levels of alumina. The normalized mass loss of V is shown in Fig. 4(a) for interpretative purposes for a curing time fixed at 7 days and a curing temperature fixed at 75°C. Contour plots of $NML(\mathrm{V})$ projected onto the matrix–concentration plane are shown in Fig. 4(b).

At high leachate pH, V in solution exists predominantly as orthovanadate ion $[VO_4]^{3-}$. Low normalized mass losses of V in OPC may be related to the formation in the matrix of a relatively stable compound such as calcium hydroxyvanadate ($Ca_5[VO_4]_3OH$) which is isostructural with calcium hydroxyapatite ($Ca_5[PO_4]_3OH$). Apatite was found by Heimann and Hooton [14] in

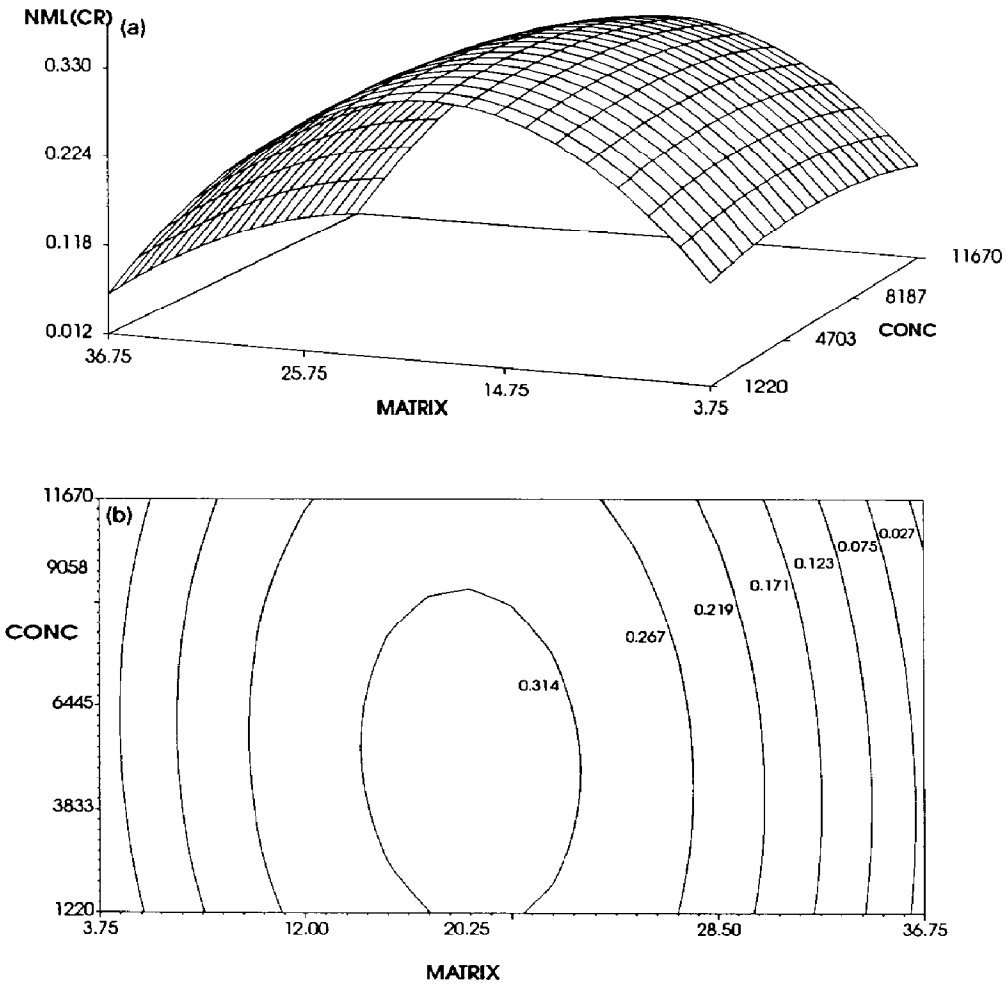

Fig. 2. Graphical representation of the regressions on response surfaces. (a) NML(Cr) upon matrix (X_1) and concentration (X_2) with curing temperature (X_3) fixed at 25 °C and curing time (X_4) fixed at 8 days. (b) Contour plot of NML(Cr) projected onto the matrix (X_1) – concentration (X_2) plane.

copious quantities during leaching of SRPC + silica fume, in contact with P_2O_5-containing Ca-bentonite, in groundwater at elevated temperatures. High pH stabilizes apatite in natural waters. At pH 12 the total soluble phosphate is limited to 0.1 ppb [15].

Both Cr and V exhibited strong mobility responses to varying levels of Al_2O_3, (Figs. 2(a), 3(a) and 4(a)) which, in turn, was related to interactions associated with varying pH in leachates (Fig. 1). Results from these analyses lead us to conclude that the predominant effect in our experiments which influenced both normalized mass losses of Cr and V, as well as pH development, was the type of cement containment matrix, characterized by varying alumina contents.

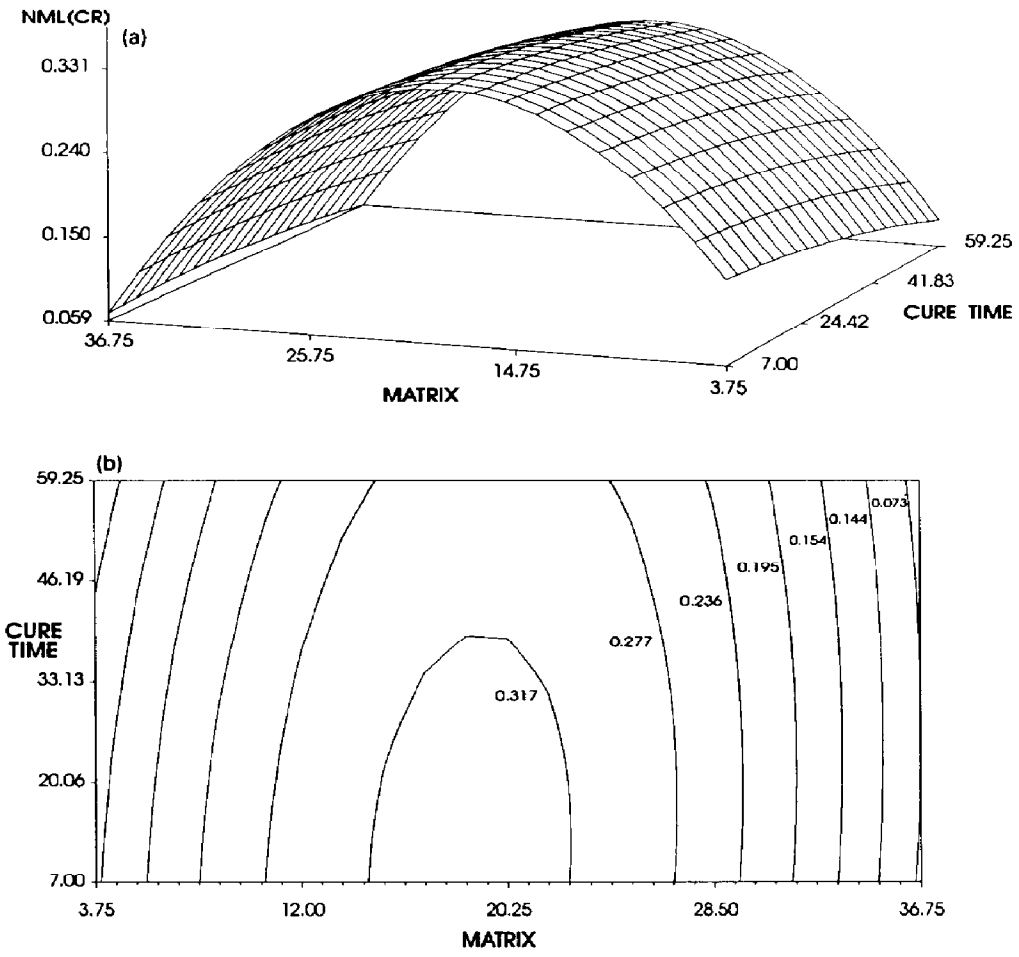

Fig. 3. Graphical representation of the regression on response surfaces. (a) $NML(\mathrm{Cr})$ upon matrix (X_1) and curing time (X_4), with concentration (X_2) fixed at 5157 mg/l and curing temperature fixed at 17°C. (b) Contour plot of $NML(\mathrm{Cr})$ in the matrix (X_1)-curing time (X_4) plane.

3.3 Transmission electron microscopy/scanning transmission electron microscopy results

Two samples, i.e. 0.4 *M* vanadium in OPC cured at 25°C for 36 days (Trial #53) and 0.1 *M* vanadium in AC cured at 50°C for 36 days (Trial #29), have been studied thus far. These samples, which were examined in both the leached and unleached conditions, were chosen because they represented the two extremes in terms of normalized mass loss of V. Trial #53 had one of the lowest V losses (10^{-3} kg/m^2), while Trial #29 had one of the highest mass losses (3.6 10^{-2} kg/m^2).

There was virtually no difference between unleached and leached samples in the TEM/STEM analysis. This is not surprising since TEM specimens, prepared from leached material, were machined from the interior of the sam-

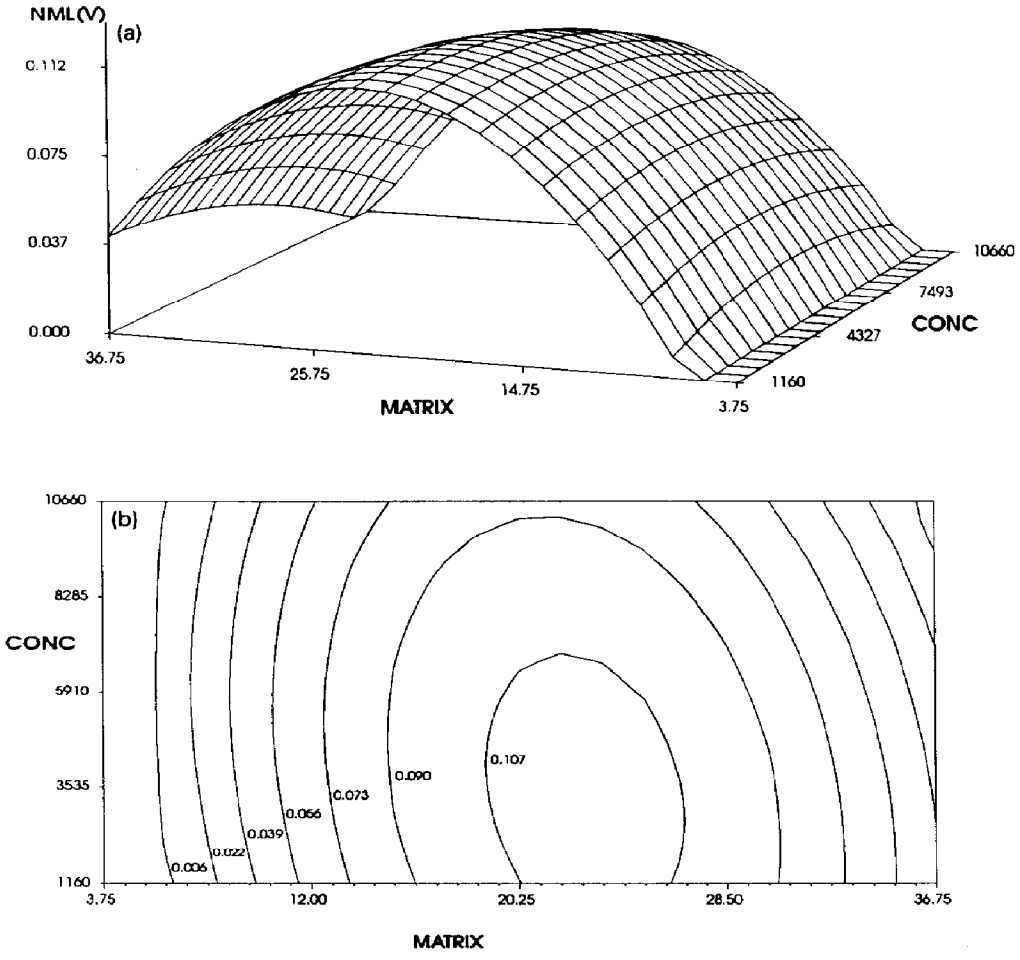

Fig. 4. Graphical representation of the regression on response surface. (a) $NML(V)$ upon matrix (X_1) and concentration (X_2) with curing temperature (X_3) fixed at 75°C and curing time (X_4) fixed at 7 days. (b) Contour plot of $NML(V)$ in the matrix (X_1)-concentration (X_2) plane.

ples and not from the surface. The interior region was not likely to be exposed to the leaching solution, at least not to the degree that the surface was. Hence, the so-called leached TEM specimens were effectively unleached.

In the Trial #53 sample, vanadium appeared to be relatively uniformly distributed throughout the matrix and was detected in low levels in calcium–silicate–hydrate (C–S–H[3]) and hydration products of calcium aluminoferrites (C_3A and C_4AF), such as ettringite. Vanadium, however, was not detected in the crystalline hydration products, such as calcium hydroxide — $Ca(OH)_2$ — or calcium carbonate ($CaCO_3$), nor was it concentrated anywhere within the hydrated paste. This last observation was different from results reported pre-

[3]Cement chemistry notation: C = CaO; A = Al_2O_3; S = SiO_2; H = H_2O; and F = Fe_2O_3.

viously for a similar system, i.e. the incorporation of trivalent Cr in OPC [7]. Calcium–chromium-rich crystalline precipitates were detected in Cr-containing hydrated pastes. However, there appeared to be some correlation between the TEM results here and the leaching analysis. The *NML*(V) from OPC was quite low while the pH was quite high ($\cong 12$). A high pH corresponds to dissolution of $Ca(OH)_2$, which was found not to contain V. Also, there was a positive correlation between the concentration of V in the leaching solution

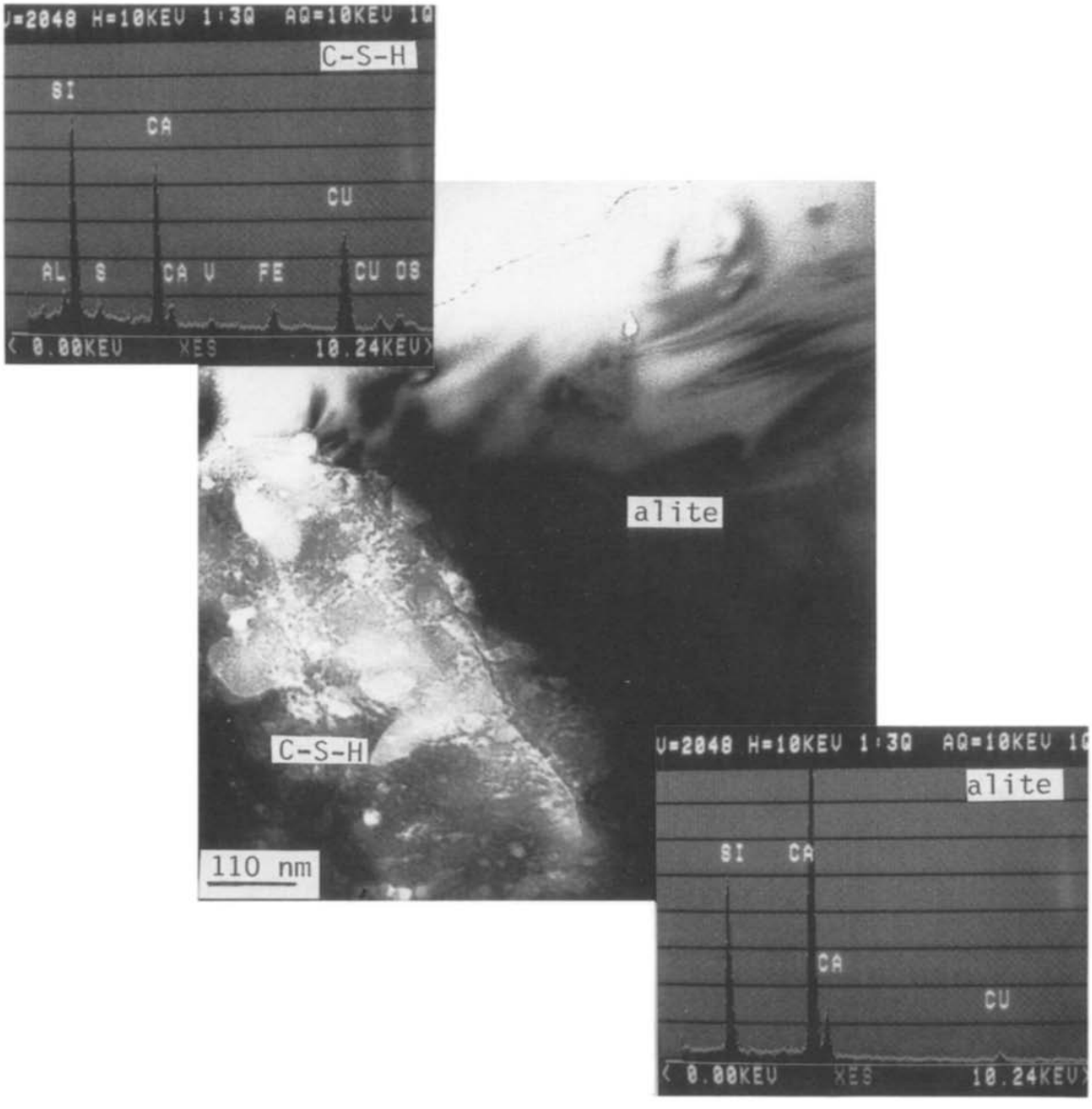

Fig. 5. Bright field TEM micrograph and X-ray spectra of a partially hydrated region of alite (C_3S) (Trial #53). The X-ray spectrum, from the C–S–H phase indicates very low levels of V.

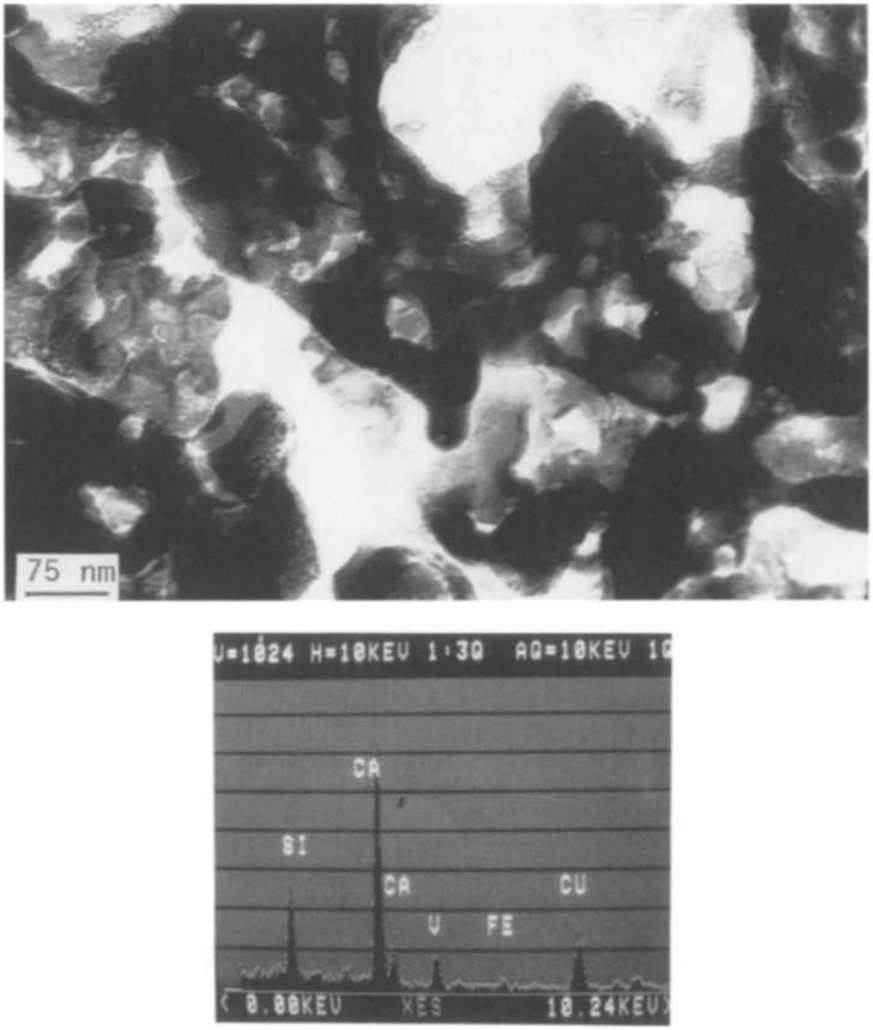

Fig. 6. Bright field TEM micrograph of an amorphous C–S–H region (Trial #53) with a representative X-ray spectrum. Note, the presence of a significant amount of V.

and the concentration of Si in the leaching solution, but no correlation between V and Ca concentrations. This suggests that V is associated with leachable Si-rich phases, i.e. C–S–H, but not with leachable Ca-rich phases, i.e. $Ca(OH)_2$ or $CaCO_3$.

The most abundant hydration phase observed was, by far, C–S–H which was expected since it makes up 60–70% of hydrated OPC pastes. Also, crystalline regions tended to sputter at lower rates than amorphous regions, which would account for the higher proportion of electron transparent areas of amorphous phases. This may also account, somewhat, for the fact that V was not detected in any crystalline phases. An example of a partially hydrated region of alite is shown in Fig. 5 (from Trial #53). The crystalline alite phase contains no V,

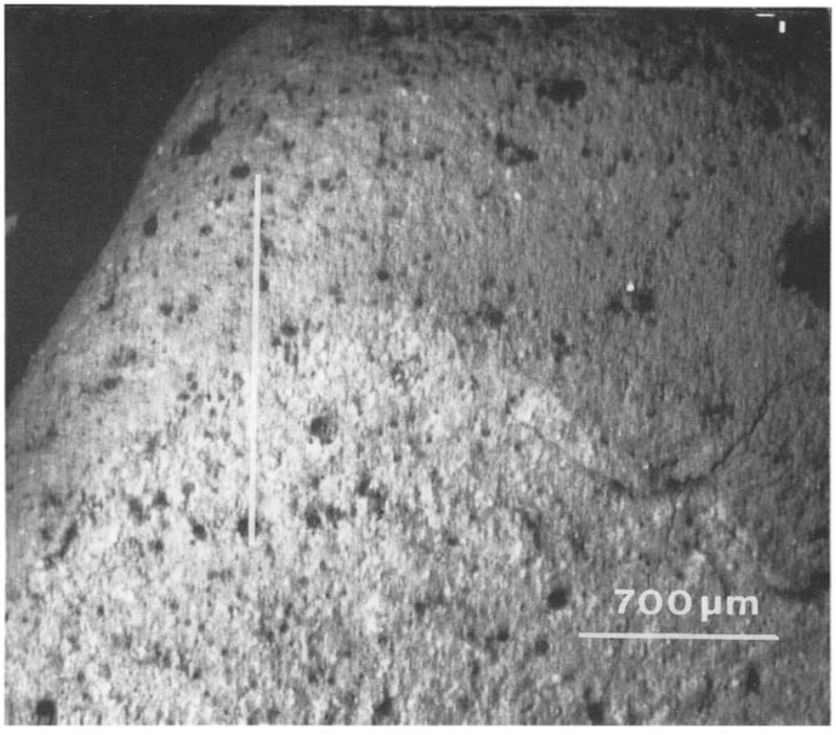

Fig. 7. Backscattered electron image of a leached, fractured cement particle (Trial #12). The fracture has exposed the relatively higher Cr content interior, which appears brighter due to a higher average atomic number than the leached exterior. The linescan region corresponding to Fig. 9 is shown.

while the C–S–H phase is amorphous and contains V levels which are barely detectable above the background level of the X-ray spectrum (Fig. 5). Other C–S–H regions with significantly higher concentrations of V were observed. One such area is shown in Fig. 6, along with a representative X-ray spectrum.

Similar behavior was observed for Trial #29 (AC). Vanadium was detected in low levels in hydration products of Ca, C_3A, C_4AF and C_2S, such as CAH_5, CAH_{10}, Afm phase $C_2(AF)H_8$, hydrogarnet $C_3(AF)H_6$ and C–S–H. Again, as with Trial #53, V-rich phases were not detected. However, this does not preclude their existence, in either OPC or AC, since the regions observed in TEM/STEM are quite small relative to the size of the hydrated samples. Consequently, the aforementioned calcium hydroxyvanadate may have been present in the OPC, but went undetected. Electron paramagnetic resonance (EPR) spectroscopy investigations of unleached and leached V-containing cement samples have been initiated, which may help to clarify the nature of V retention.

3.4 Scanning electron microscopy results

Figure 7 shows a backscattered electron image of a leached cement which originally contained 1.0 *M* Cr (Trial #12). It has been fractured and in this

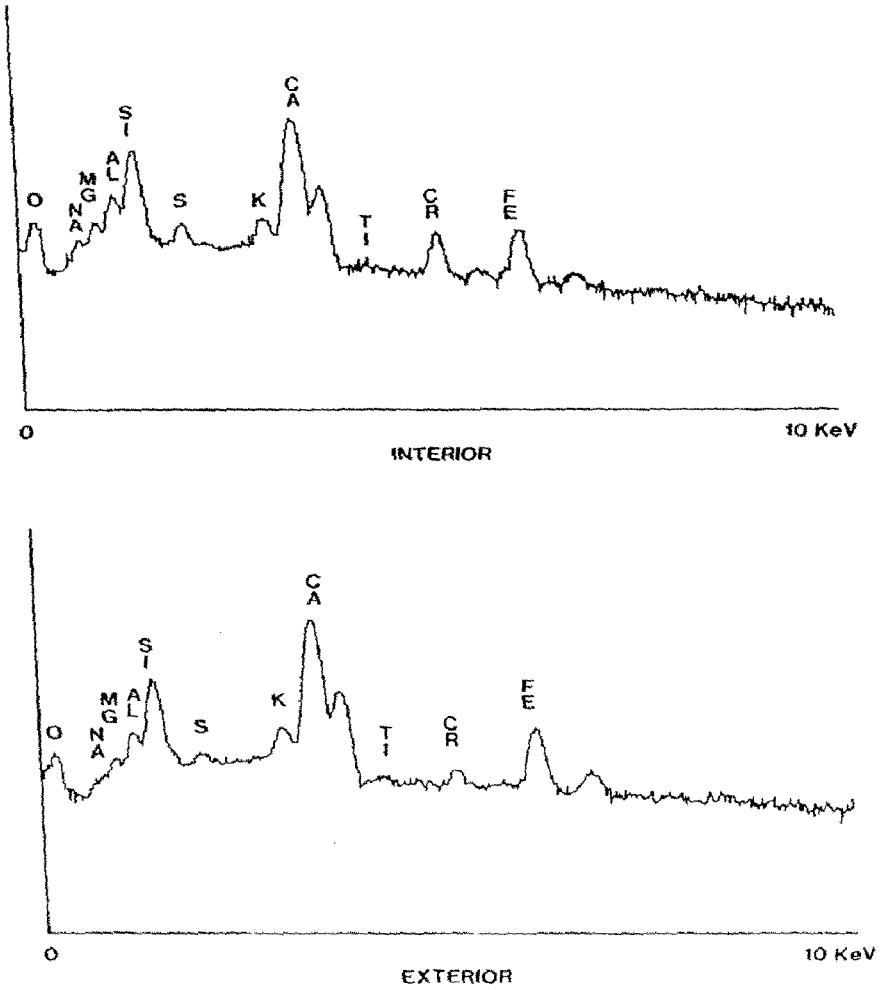

Fig. 8. X-ray spectra (displayed on a log scale) of the interior and exterior areas of the leached cement (Trial #12), which illustrate the significant decrease in Cr (and S) content at the cement surface due to leaching. The spectra were acquired at 25 kV and 0.2 nA for 200 s.

particular orientation both the interior and exterior surfaces can be observed. The relatively brighter interior region has a higher concentration of Cr than the more severely leached exterior surface. The X-ray spectra of the interior and exterior surfaces (Fig. 8) illustrate this difference, as does the linescan in Fig. 9, which has both Cr and Fe peak heights displayed. The Fe content is constant, indicating that the decrease in Cr X-ray intensity is not due to sample topography or to beam current fluctuations. The peaks and valleys in Cr and Fe concentration are due to localized regions of high Cr or Fe. The data in both Figs. 8 and 9 were taken with a 25 kV incident electron beam and approx-

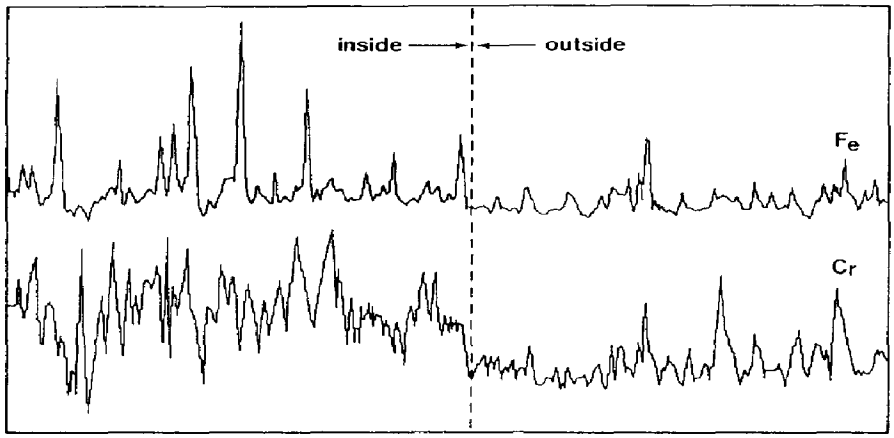

Fig. 9. X-ray linescan across the interior/exterior fracture boundary of Fig. 7, showing the distinct decrease in Cr on the exterior surface of the leached cement. The linescan was acquired over 256 points, corresponding to the line (1600 μm) in Fig. 7. The X-ray intensities were determined from the K_α lines of Cr and Fe, acquired at 25 kV, 0.2 nA and 20 s/point.

imately 0.2 nA beam current. With an appropriate choice of standards and careful sample preparation, it might be possible to relate leaching data to the loss of Cr from specific cement regions or to quantify metal loss from regions of the cement sample.

4. Conclusions

Leaching performed on samples of heavy metal waste (Cr, V, Cd) solidified/stabilized in cementitious matrices (OPC, SRPC+FA and AC) showed that:

(1) Cd is effectively retained in all cements and shows no sensitivity to leachate pH.
(2) Both NML of Cr and V are maximized at intermediate levels of alumina in the cement matrix and minimized at high and low alumina contents. This is related to the amphoteric nature of the Al.

Acknowledgements

The patience and dedicated assistance of the following individuals: Rosemary Harris, Arlene Oatway, Lyle Voltner, Philip J. Henry, John Kirtz, Ed Zacharuk and the late Donald Klick, are respectfully acknowledged.

References

1 P. Bishop, D.L. Gress and J.A. Olofsson, In: J.E. Alleman and J.T. Kavanagh (Eds.), Proc. 14th Mid-Atlantic Ind. Waste Conf., Ann Arbor Science, Ann Arbor, MI, 1982, pp. 459-467.

2 P. Bishop, S.B. Ransom and D.L. Gress, Proc. Ind. Waste Conf., Purdue University, Lafayette, IN, 1983, pp. 395–401.
3 P. Bishop, Hazard. Waste Hazard. Mater., 5 (1988) 129–143.
4 G.J. de Groot, J. Wijkstra, D. Hoede and H.A. van der Sloot, In: P.L. Cote and T.M. Gilliam, (Eds.), In: Environmental Aspects of Stabilization and Solidification of Hazardous and Radioactive Wastes, ASTM STP 1033, ASTM, Philadelphia, PA, 1989, pp. 170–183.
5 C.S. Poon, A.I. Clark and R. Perry, Cem. Concr. Res., 16 (1986) 161–172.
6 W. Shively, W. Bishop, F. Gress and T. Brown, J. Water Pollut. Control Fed., 58 (1986) 234–241.
7 D.G. Ivey, M. Neuwirth, S. Shumborski, D. Conrad, R.J. Mikula, W.W. Lam and R.B. Heimann, J. Mater. Sci., 25 (1990) 5055–5062.
8 M. Neuwirth, R. Mikula and P. Hannak, In: P.L. Cote and T.M. Gilliam (Eds.), Environmental Aspects of Stabilization and Solidification of Hazardous and Radioactive Wastes, ASTM STP 1033, ASTM, Philadelphia, PA, 1989, pp. 201–213.
9 C.S. Poon, C.J. Peters and R. Perry, Sci. Total Environ., 41 (1985) 55–71.
10 U.S. Environmental Protection Agency, Federal Register, Washington, DC, 51 (114) (1986) 21 685–21 688.
11 G.E.P. Box and D.W. Behnken, Technometrics, 2 (4) (1960) 455–475.
12 SAS Institute Inc., SAS/STAT User's Guide, Release 6.03 Edition, SAS Institute Inc., Cary, NC, 1988, 1028 pp.
13 J.E. Mendel, Nuclear Waste Materials Handbook of Test Methods, DOE/T1C-11400, published by Pacific Northwest Laboratories, Richland, WA, 1983, pp. 1–11.
14 R.B. Heimann and R.D. Hooton, Can. Mineralog., 24 (1986) 289–302.
15 W. Stumm and J.J. Morgan, Aquatic Chemistry, Wiley-Interscience, New York, NY, 1970, pp. 522–523.